

## Determination of cancellous bone density using low frequency acoustic measurements

Robert P. Gilbert\*, Philippe Guyenne and George C. Hsiao

*Department of Mathematical Sciences, University of Delaware, Newark, DE, USA*

*(Received 12 May 2008; final version received 13 May 2008)*

In this article we offer a novel method for interrogating cancellous bone using ultra sound measurements. The problem is first modelled in terms of the acoustic pressure in the water bath surrounding the bone sample, the pore pressure and the displacement of the elastic matrix describing the cancellous bone specimen. The fluid pressure in the water tank is represented in terms of a boundary integral equation. Source points are placed on a parallel line on one side of the bone; whereas, receivers are placed on the other side of the bone. Sensitivity tests are run for two frequencies which show that the corresponding inverse problem leads to reasonable good results.

**Keywords:** inverse problems; cancellous bone; ultrasound

### 1. Introduction

Cancellous bone is a two component material consisting of a calcified bone matrix with interspinal fatty marrow. Hence mathematical models of poroplastic media are applicable. McKelvie and Palmer [1], Williams [2], and Hosokawa and Otani [3] discussed the application of Biot's model for a poroplastic medium to cancellous bone. Use of this model requires determination of the parameters upon which it depends. This can be an expensive process. In this article we investigate whether these parameters can be ascertained by acoustic interrogation.

### 2. The Biot model applied to cancellous bone

The Biot–Stoll [4,5,6] model treats a poroplastic medium as an elastic frame with interspinal pore fluid. Cancellous bone is anisotropic, however, as pointed out by Williams, if the acoustic waves passing through it travel in the trabecular direction an isotropic model may be acceptable. We will simulate a two-dimensional version of the experiments described in McKelvie and Palmer and Hosokawa and Otani. See also in this regard [7,8]. The motion of the frame and fluid within the bone are tracked by position vectors  $\mathbf{u} = [u_1, u_2]$  and  $\mathbf{U} = [U_1, U_2]$ . The constitutive equations used by Biot are those of

---

\*Corresponding author. Email: robert.glbrt1@gmail.com

a linear elastic material with terms added to account for the interaction of the frame and interstitial fluid

$$\begin{aligned}
 \sigma_{x_1x_1} &= 2\mu e_{x_1x_1} + \lambda e + Q\epsilon, \\
 \sigma_{x_2x_2} &= 2\mu e_{x_2x_2} + \lambda e + Q\epsilon, \\
 \sigma_{x_1x_2} &= \mu e_{x_1x_2}, \quad \sigma_{x_2x_1} = \mu e_{x_2x_1}, \\
 s &= Qe + R\epsilon,
 \end{aligned}
 \tag{1}$$

where the solid and fluid dilatations are given by

$$e = \nabla \cdot \mathbf{u} = \frac{\partial u_1}{\partial x_1} + \frac{\partial u_2}{\partial x_2}, \quad \epsilon = \nabla \cdot \mathbf{U} = \frac{\partial U_1}{\partial x_1} + \frac{\partial U_2}{\partial x_2}.
 \tag{2}$$

The strains are defined by

$$e_{x_1x_1} = \frac{\partial u_1}{\partial x_1}, \quad e_{x_1x_2} = e_{x_2x_1} = \frac{\partial u_1}{\partial x_2} + \frac{\partial u_2}{\partial x_1}, \quad e_{x_2x_2} = \frac{\partial u_2}{\partial x_2}.
 \tag{3}$$

The parameter  $\mu$ , the complex frame shear modulus is measured. The other parameters  $\lambda$ ,  $R$  and  $Q$  occurring in the constitutive equations are calculated from the measured or estimated values of the parameters given in Table 1 using the formulas:

$$\begin{aligned}
 \lambda &= K_b - \frac{2}{3}\mu + \frac{(K_r - K_b)^2 - 2\beta K_r(K_r - K_b) + \beta^2 K_r^2}{D - K_b}, \\
 R &= \frac{\beta^2 K_r^2}{D - K_b}, \\
 Q &= \frac{\beta K_r((1 - \beta)K_r - K_b)}{D - K_b},
 \end{aligned}
 \tag{4}$$

where

$$D = K_r(1 + \beta(K_r/K_f - 1)).
 \tag{5}$$

The bulk and shear moduli  $K_b$  and  $\mu$  are often given imaginary parts to account for frame inelasticity. Equations (1), (2) and (3) and an argument based upon Lagrangian dynamics

Table 1. Parameters in the Biot model.

Symbol	Parameter
$\rho_f$	Density of the pore fluid
$\rho_r$	Density of frame material
$K_b$	Complex frame bulk modulus
$\mu$	Complex frame shear modulus
$K_f$	Fluid bulk modulus
$K_r$	Frame material bulk modulus
$\beta$	Porosity
$\eta$	Viscosity of pore fluid
$k$	Permeability
$\alpha$	Structure constant
$a$	Pore size parameter

are shown in [4,9] to lead to the following equations of motion for the displacements  $\mathbf{u}$ ,  $\mathbf{U}$  and dilatations  $e$ ,  $\epsilon$ :

$$\begin{aligned} \mu \nabla^2 \mathbf{u} + \nabla[(\lambda + \mu)e + Q\epsilon] &= \frac{\partial^2}{\partial t^2}(\rho_{11}\mathbf{u} + \rho_{12}\mathbf{U}) + b \frac{\partial}{\partial t}(\mathbf{u} - \mathbf{U}), \\ \nabla[Qe + R\epsilon] &= \frac{\partial^2}{\partial t^2}(\rho_{12}\mathbf{u} + \rho_{22}\mathbf{U}) - b \frac{\partial}{\partial t}(\mathbf{u} - \mathbf{U}). \end{aligned} \tag{6}$$

Here  $\rho_{11}$  and  $\rho_{22}$  are density parameters for the solid and fluid,  $\rho_{12}$  is a density coupling parameter, and  $b$  is a dissipation parameter. These are calculated from the inputs of Table 1 using the formulas:

$$\begin{aligned} \rho_{11} &= (1 - \beta)\rho_r - \beta(\rho_f - m\beta), \\ \rho_{12} &= \beta(\rho_f - m\beta), \\ \rho_{22} &= m\beta^2, \\ b &= \frac{F(a\sqrt{\omega\rho_f/\eta})\beta^2\eta}{k}, \end{aligned}$$

where

$$m = \frac{\alpha\rho_f}{\beta},$$

and the multiplicative factor  $F(\zeta)$ , which was introduced in [4] to correct for the invalidity of the assumption of Poiseuille flow at high frequencies, is given by

$$F(\zeta) = \frac{1}{4} \frac{\zeta T(\zeta)}{1 - 2T(\zeta)/i\zeta}, \tag{7}$$

where  $T$  is defined in terms of Kelvin functions:

$$T(\zeta) = \frac{\text{ber}'(\zeta) + i\text{bei}'(\zeta)}{\text{ber}(\zeta) + i\text{bei}(\zeta)}.$$

The bone specimen is assumed to oscillate harmonically in time:  $\mathbf{u}(x, y, t) = \mathbf{u}(x, y)e^{i\omega t}$ ,  $\mathbf{U}(x, y, t) = \mathbf{U}(x, y)e^{i\omega t}$ . Substituting these representations into (6) gives

$$\begin{aligned} \mu \nabla^2 \mathbf{u} + \nabla[(\lambda + \mu)e + Q\epsilon] + p_{11}\mathbf{u} + p_{12}\mathbf{U} &= 0, \\ \nabla[Qe + R\epsilon] + p_{12}\mathbf{u} + p_{22}\mathbf{U} &= 0, \end{aligned} \tag{8}$$

where

$$p_{11} := \omega^2 \rho_{11} - i\omega b, \quad p_{12} := \omega^2 \rho_{12} + i\omega b, \quad p_{22} := \omega^2 \rho_{22} - i\omega b. \tag{9}$$

### 3. Boundary value problem

A bone specimen is placed in a water tank. The region occupied by the bone specimen and the water are  $\Omega^b$  and  $\Omega^w$ , respectively. In  $\Omega^w$ , we have in the two-dimensional

case the differential equations for fluid pressure  $P$  and the fluid displacement  $\mathbf{U}^w := (U_1^w, U_2^w)$ , i.e.

$$-\nabla^2 P - k_0^2 P = -q \delta(\mathbf{x}; \mathbf{x}_0; k_0), \tag{10}$$

$$\nabla P - \rho^w \omega^2 \mathbf{U}^w = q \nabla_{\mathbf{x}} \Gamma(\mathbf{x}, \mathbf{x}_0, k_0), \tag{11}$$

where  $\Gamma(\mathbf{x}, \mathbf{x}_0, k_0)$  is the harmonic Green's function with a fixed source point located at  $\mathbf{x}_0 = (x_0, y_0)$ ; see the Appendix, Equation (31).

In the bone specimen  $\Omega^b$ , in order to formulate a well-posed boundary value problem, one must modify the present form of the Biot Equation (8), since there are not enough transmission conditions for the components of displacements fields  $u_1, u_2, U_1$  and  $U_2$ . The main idea here is to replace the unknowns  $U_1$  and  $U_2$  by a single known  $s$  in the equations. To see this, we first express  $\epsilon$  and  $\mathbf{U}$  in terms of  $s$  from (1) and (8),

$$\epsilon = \frac{1}{R}(s - Q e), \quad \mathbf{U} = -\frac{1}{p_{22}}(\nabla s + p_{12} \mathbf{u}). \tag{12}$$

By taking the divergence of the second equation of (8), we obtain

$$\nabla^2 s + p_{12} e + p_{22} \epsilon = 0,$$

which reduces to

$$\nabla^2 s + \frac{p_{22}}{R} s + \left( p_{12} - \frac{p_{22} Q}{R} \right) e = 0, \tag{13}$$

by making use of (12). Similarly, the first equation of (8) can be written in the form:

$$\mu \nabla^2 \mathbf{u} + \nabla \left[ \left( \lambda + \mu - \frac{Q^2}{R} \right) e + \left( \frac{Q}{R} - \frac{p_{12}}{p_{22}} \right) s \right] + \left( p_{11} - \frac{p_{12}^2}{p_{22}} \right) \mathbf{u} = 0. \tag{14}$$

Equations (13) and (14) then form the modified Biot equations for  $\mathbf{u}$  and  $s$  in the bone specimen  $\Omega^b$ . These equations should be satisfied by  $\mathbf{u}$  and  $s$  together with boundary conditions on the interface between bone and water. These are:

- Continuity of the flux: From (11)

$$\rho^w \omega^2 (\beta \mathbf{n} \cdot \mathbf{U} + (1 - \beta) \mathbf{n} \cdot \mathbf{u}) = \rho^w \omega^2 \mathbf{n} \cdot \mathbf{U}^w \equiv \mathbf{n} \cdot (\nabla P - q \nabla_{\mathbf{x}} \Gamma(\mathbf{x}, \mathbf{x}_0)),$$

and thus

$$\rho^w \omega^2 \left( \left[ 1 - \beta \left( 1 + \frac{p_{12}}{p_{22}} \right) \right] \mathbf{n} \cdot \mathbf{u} - \frac{\beta}{p_{22}} \frac{\partial s}{\partial n} \right) - \mathbf{n} \cdot (\nabla P - q \nabla_{\mathbf{x}} \Gamma(\mathbf{x}, \mathbf{x}_0)) = 0. \tag{15}$$

Here  $\mathbf{n}$  is the exterior normal to  $\Omega^b$ , which points into the water.

- Continuity of the aggregate pressure

$$\sigma_{\ell,j} n_j + s n_{\ell} = -P n_{\ell}, \tag{16}$$

since an expansion of the bone induces a compression in the water. Here  $\sigma_{\ell,j} = \sigma_{x_{\ell} x_j}$  denotes the components of the stress tensor in (1).

- Continuity of pore pressure:

$$s = -\beta P. \tag{17}$$

- Vanishing of the tangential frame stress  $\sigma_{12} \equiv \sigma_{21} = 0$  which is equivalent to

$$\frac{\partial u_1}{\partial x_2} + \frac{\partial u_2}{\partial x_1} = 0. \tag{18}$$

In addition, it is understood that the pressure  $P$  is also required to satisfy the two-dimensional Sommerfeld radiation condition at infinity. We have so far giving the precise formulation of the exterior transmission problem (ETP) consisting of the partial differential Equations (13 and 14) for the unknowns  $\mathbf{u}$ ,  $s$  in  $\Omega^b$  and the Equation (10) for the unknown  $P$  in  $\Omega^w$  together with transmission conditions (15–18) and the radiation condition at infinity.

From the computational point of view, it is more convenient to reduce the problem (ETP) to a non-local problem in a finite computational domain such as  $\Omega^b$ . For this purpose, we now reduce the Helmholtz Equation (10) to a boundary integral equation by using the Green representation of  $P$  in  $\Omega^w$ . More precisely, we seek a solution of (10) in the form of a simple-layer potential in terms of the unknown density function  $\varphi$ :

$$P(\mathbf{x}, \mathbf{x}_0) := -q G(\mathbf{x}, \mathbf{x}_0; k_0) - \int_{\partial\Omega^b} G(\mathbf{x}, \zeta; k_0)\varphi(\mathbf{x}_0, \zeta)ds_\zeta, \quad \mathbf{x} \in \Omega^w,$$

where  $G(\mathbf{x}, \mathbf{x}_0, k_0)$  is free-space Helmholtz–Green’s function given by

$$G(\mathbf{x}, \mathbf{x}_0, k_0) := \frac{i}{4} H_0^{(1)}(k_0 \|\mathbf{x} - \mathbf{x}_0\|),$$

with  $\mathbf{x} = (x, y)$ ,  $\mathbf{x}_0 = (x_0, y_0)$ . (See Appendix Equation (33).) Clearly, the unknown density function  $\varphi$  is related to the unknowns  $\mathbf{u}$  and  $\mathbf{U}$  via the transmission conditions (15–18).

If the bone sample,  $\partial\Omega^b$ , has positive orientation, then letting  $\mathbf{x} \rightarrow \mathbf{X} \in \partial\Omega^b$  we obtain from condition (16) that

$$\left( \lambda \nabla \cdot \mathbf{u} + 2\mu \frac{\partial u_1}{\partial x_1} + Q\epsilon \right) + s = q G(\mathbf{X}, \mathbf{x}_0; k_0) + \int_{\partial\Omega^b} G(\mathbf{X}, \zeta; k_0)\varphi(\mathbf{x}_0, \zeta)ds_\zeta, \tag{19}$$

and

$$\left( \lambda \nabla \cdot \mathbf{u} + 2\mu \frac{\partial u_2}{\partial x_2} + Q\epsilon \right) + s = q G(\mathbf{X}, \mathbf{x}_0; k_0) + \int_{\partial\Omega^b} G(\mathbf{X}, \zeta; k_0)\varphi(\mathbf{x}_0, \zeta)ds_\zeta. \tag{20}$$

Note that in deriving these equations, we have tacitly employed the condition (18). In view of the similarity of the Equations (19) and (20), a subtraction of the two equations leads to the simple relation:

$$\frac{\partial u_1}{\partial x_1} - \frac{\partial u_2}{\partial x_2} = 0. \tag{21}$$

Hence in computation, we may use (21) and either (19) or (20), but not both. Here the term  $\epsilon$  should be replaced by  $\epsilon = (1/R)(s - Qe)$  in (12).

Next, the flux continuity condition (15) leads to the natural boundary condition for  $s$ :

$$\begin{aligned} & \rho^w \omega^2 \left( \left[ 1 - \beta \left( 1 + \frac{p_{12}}{p_{22}} \right) \right] \mathbf{n} \cdot \mathbf{u} - \frac{\beta}{p_{22}} \frac{\partial s}{\partial n} \right) + q \frac{\partial}{\partial \mathbf{n}_X} (G(\mathbf{X}, \mathbf{x}_0; k_0) + \Gamma(\mathbf{X}, \mathbf{x}_0, k_0)) \\ & = \frac{1}{2} \varphi(\mathbf{x}_0, \mathbf{X}) - \int_{\partial \Omega^b} \varphi(\mathbf{x}_0, \zeta) \frac{\partial G(\mathbf{X}, \zeta; k_0)}{\partial \mathbf{n}_X} ds_\zeta. \end{aligned} \quad (22)$$

Finally, from the representation formula for  $P$ , the condition (17) leads to a boundary integral equation for  $\varphi$ :

$$\beta \int_{\partial \Omega^b} G(\mathbf{X}, \zeta; k_0) \varphi(\mathbf{x}_0, \zeta) ds_\zeta - s + \beta q G(\mathbf{X}, \mathbf{x}_0; k_0) = 0. \quad (23)$$

It is worthy mentioning that the right-hand sides of all the Equations (19), (20), (22) and (23) contain no singularities, since for the first three equations the source point  $\mathbf{x}_0$  is in  $\Omega^b$ , whereas for Equation (22), the singularity is cancelled, because of the last term on the right-hand side.

Before we formulate what is called *the non-local problem* for ETP, some observations are in order. We observe that the transmission conditions (19) and (20) can be considered as natural boundary conditions for the displacement fields  $\mathbf{u}$  for given  $s$  and  $\varphi$ , whereas condition (22) is a natural condition for the stress  $s$ , if  $\mathbf{u}$  and  $\varphi$  are known. From the variational formulation point of view, both equations define the relevant Dirichlet–Neumann maps. On the other hand, the condition (23) only relates the trace of the stress  $s$  and the known density function  $\varphi$ , which may be considered as a boundary integral equation for  $\varphi$  for the given stress  $s$ . With these observations, we are now in a position to state **the non-local problem** for (ETP):

*Find the four unknowns  $u_1$ ,  $u_2$ ,  $s$ ,  $\varphi$ . The first three unknowns are required to satisfy the Biot equations (13–14) and the boundary conditions (or rather the transmission conditions) either (19) or (20), (21) and (22), where the density  $\varphi$  may be considered as an unknown parameter subject to the constraint (23).*

We note that if  $\varphi$  is given, then we have an uncoupled system for displacement fields  $u_1$ ,  $u_2$ ,  $s$ . On the other hand, if the displacement fields  $u_1$ ,  $u_2$  and the stress  $s$  are known, then the unknown density function  $\varphi$  is required to satisfy the standard Fredholm boundary integral equation of the first kind (23). In general this is a coupled system for the five unknowns, and can only be treated by numerical methods, which is the content of the next section.

#### 4. Numerical approximation

We consider the simple situation where the bone specimen is a square of dimension  $L \times L$ . The domain is discretized into a uniform Cartesian grid consisting of  $N \times N$  points. We solve the coupled system of equations (13), (14), (19), (21) (or (20), (21)), (22) and (23) by using a finite-difference method.

More specifically, the derivatives in the equations are approximated by 2nd-order finite-difference schemes: central difference schemes are used for the bulk equations, while backward or forward difference schemes are used for the boundary conditions (depending on the square's edge or corner under consideration). An exception is made for the discretization of the tangential derivatives along the edges, which are approximated only by 1st-order backward difference schemes. This choice is motivated by two reasons: to keep the

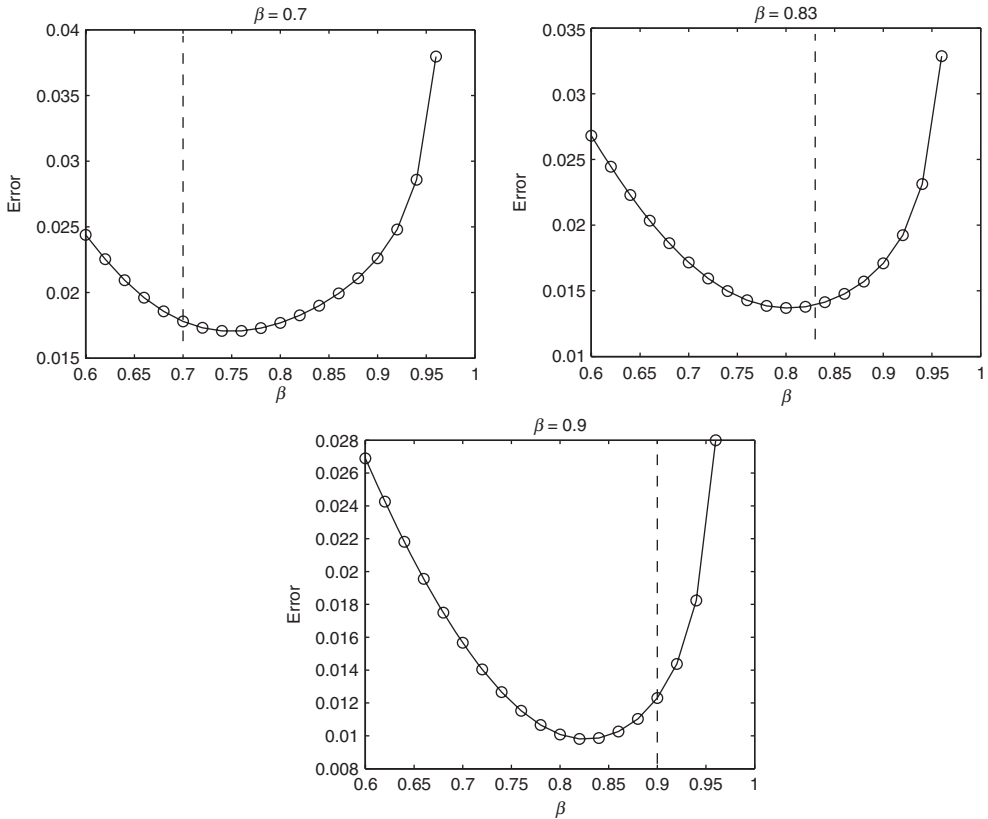


Figure 1. Relative error on  $P$  for  $\beta=0.7, 0.83, 0.9$  and  $\omega=2\pi \times 10^4$ .

implementation relatively simple (as compared to 2nd-order backward/forward formulas which would require special treatment near corners) and to avoid solving a badly ill-conditioned linear system (as compared to 2nd-order central formulas which would imply having zeros on the main diagonal of the resulting coefficient matrix).

The quadrature of the boundary integrals in (19) (or (20)), (22) and (23) is based on constant interpolation of the solution between grid points, which gives a reasonably good approximation given the simple geometry of the problem. For simplicity  $H=0$  in  $\Gamma$ . Finally, the resulting linear system is solved by a direct method (Gaussian elimination).

As an example, for a point  $\mathbf{X}(j, l)$  located on the left edge of the bone specimen (except the corners), the discretized form of (19) is given by

$$\begin{aligned}
 & \left( \lambda + 2\mu - \frac{Q^2}{R} \right) \left[ -u_1(j+2, l) + 4u_1(j+1, l) - 3u_1(j, l) \right] \\
 & + 2 \left( \lambda - \frac{Q^2}{R} \right) \left[ u_2(j, l) - u_2(j, l-1) \right] + 2\Delta x \left( 1 + \frac{Q}{R} \right) s(j, l) \\
 & = 2q \Delta x G(\mathbf{X}, \mathbf{x}_0; k_0) + 2 \sum_{\zeta \in \partial\Omega^b} G(\mathbf{X}, \zeta; k_0) \varphi(\mathbf{x}_0, \zeta) (\Delta x)^2,
 \end{aligned} \tag{24}$$

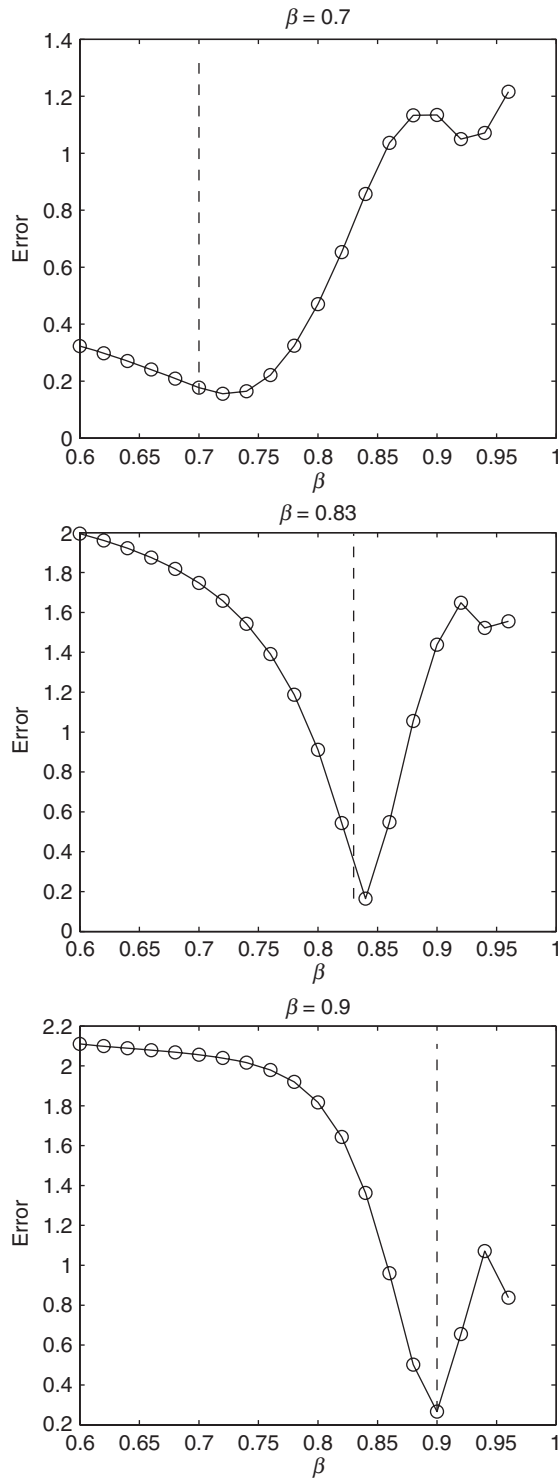


Figure 2. Relative error on  $P$  for  $\beta=0.7, 0.83, 0.9$  and  $\omega=2\pi \times 5 \times 10^4$ .



where

$$G(\mathbf{X}, \zeta; k_0) = \begin{cases} \frac{i}{4} H_0^{(1)}(k_0 \|\mathbf{X} - \zeta\|) & \text{if } \mathbf{X} \neq \zeta, \\ \frac{i}{8\pi} \Delta x \left[ \log\left(\frac{2}{\Delta x}\right) + 1 \right] & \text{if } \mathbf{X} = \zeta, \end{cases} \tag{25}$$

and  $\Delta x$  is the grid spacing.

**5. Numerical experiments**

To validate the model, we perform a sensitivity test on the parameter  $\beta$  (porosity). More precisely, for a given  $\beta$ , we compute the pressure  $P$  at 11 receiving points outside the bone specimen, and we do so for different resolutions in order to compare the results. We should mention that, in clinical practice, it would be possible to wrap the member with a series of receiving and source points which would lead to a more accurate determination of the porosity. The center of the square (bone specimen) is located at  $x_1 = x_2 = 5L/2$ , a single source is positioned at  $x_1 = L, x_2 = 5L/2$  and the receiving points are positioned at  $x_1 = 4L$ , equally spaced between  $L \leq x_2 \leq 4L$ .

The physical parameters we use are (in dimensional units):  $L = 0.01, \rho_f = 950, \rho_r = 1960, K_f = 2 \times 10^9, K_r = 2 \times 10^{10}, \eta = 1.5$  and  $a = 0.001$ . For the sensitivity test, the reference high resolution is  $N = 41$  and this is compared with simulations of lower resolution  $N = 25$ . The comparison is performed by computing the relative error on  $P$  between the two resolutions and over the 11 receiving points, i.e.

$$\text{Error} = \frac{\left[ \sum_{j=1}^{11} (P_j^{41} - P_j^{25})^2 \right]^{1/2}}{\left[ \sum_{j=1}^{11} (P_j^{41})^2 \right]^{1/2}}, \tag{26}$$

where  $P^{25}$  and  $P^{41}$  are the pressures for resolutions  $N = 25$  and  $N = 41$ , respectively.

Figure 1 shows the results for  $\beta = 0.7, 0.83, 0.9$  and  $\omega = 2\pi \times 10^4$ , while Figure 2 shows the results for the same set of  $\beta$  but a larger frequency  $\omega = 2\pi \times 5 \times 10^4$ . In Figure 1, the reference  $\beta$ 's do not coincide exactly with the minimum of the curves but the values are nevertheless relatively close. The agreement becomes better as  $\omega$  increases, especially for large  $\beta$  (Figure 2). The results would certainly improve if higher resolutions were used. However we could not specify resolutions much larger than  $N = 41$  due to the memory limitations of our computer. Overall the outcome of the sensitivity test on  $\beta$  is satisfactory.

The comparison of the results of the two frequencies also suggests that there are so-called good frequencies and bad frequencies. Choosing a pulsed signal would allow many frequencies to be used and the appropriated weighted norm could also be tried. We believe this to be the case and that is the purpose of a future investigation.

**Acknowledgements**

R.P. Gilbert was supported in part by the NSF through grant No. INT-0438765. P. Guyenne was supported in part by the University of Delaware Research Foundation and the NSF through grant No. DMS-0625931.

## References

- [1] M.L. McKelvie and S.B. Palmer, *The interaction of ultrasound with cancellous bone*, Phys. Med. Biol. 10 (1991), pp. 1331–1340.
- [2] J.L. Williams, *Prediction of some experimental results by Biot's theory*, J. Acoust. Soc. Am. 91 (1992), pp. 1106–1112.
- [3] A. Hosokawa and T. Otani, *Ultrasonic wave propagation in bovine cancellous bone*, J. Acoust. Soc. Am. 101 (1997), pp. 558–562.
- [4] M.A. Biot, *Theory of propagation of elastic waves in a fluid-saturated porous solid. I. Lower frequency range, and II. Higher frequency range*, J. Acoust. Soc. Am. 28 (1956), pp. 68–78, 79–9.
- [5] —, *Mechanics of deformation and acoustic propagation in porous media*, J. Appl. Phys. 33 (1962), pp. 482–498.
- [6] R.D. Stoll, *Acoustic waves in saturated sediments*, in *Physics of Sound in Marine Sediments*, L. Hampton, ed., Plenum, New York, 1974, pp. 19–39.
- [7] J.L. Buchanan, R.P. Gilbert, and K. Khashanah, *Determination of the parameters of cancellous bone using low frequency acoustic measurements*, J. Comput. Acoust. 12 (2004), pp. 99–126.
- [8] J.L. Buchanan et al., *Transient reflection and transmission of ultrasonic waves in cancellous bones*, Math. Comput. Model. 142 (2003), pp. 561–573.
- [9] J.L. Buchanan et al., *Marine Acoustics: Direct and Inverse Problems*, SIAM, Philadelphia, 2004.
- [10] G.C. Hsiao and W.L. Wendland, *Boundary Integral Equations, Series: Applied Mathematical Sciences (AMS)*, Vol. 164, Springer, Berlin, 2008.
- [11] —, *Boundary integral equations in low frequency acoustics*, J. Chin. Inst. Eng. 23 (2000), pp. 369–375.
- [12] S. Chaffai et al., *In vitro measurement of the frequency dependent attenuation in cancellous bone between 0.2 and 2 MHz*, J. Acoust., Soc. Amer. 108 (2000), pp. 1281–1289.
- [13] M. Fang et al., *Numerical homogenizing the time harmonic acoustics of bone: the monophasic case*, Int. J. Multiscale Comp. Eng. 5 (2007), pp. 461–472.
- [14] N.L. Fazzalari, D.J. Crisp, and B. Vernon-Roberts, *Mathematical modeling of trabecular bone structure: the evaluation of analytical and quantified surface to volume relationships in the femoral head and iliac crest*, J. Biomech. 22 (1989), pp. 90–100.
- [15] P.R. Garabedian, *Partial Differential Equations*, John Wiley, New York, 1964.
- [16] T. Hildebrand and P. Rügsegger, *Quantification of bone architecture with structure model index*, Comput. Math. Biomech. Biomed. Eng. 1 (1997), pp. 5–23.
- [17] E.R. Hughes et al., *Ultrasonic propagation in cancellous bone: A new stratified model*, Ultrasound in Med. & Biol. 25 (1999), pp. 811–821.
- [18] H. Jinnai et al., *Surface curvature of trabecular bone microarchitecture*, Bone 30 (2002), pp. 191–194.

## Appendix

### Gradient of the pressure

To derive the correct integral equations which describe our problem, we must first go back to the interaction with fluid and poro-elastic solid equations. In the fluid we have the Navier–Stokes equations holding for  $\mathbf{V} = \mathbf{U}$

$$\rho^w \frac{\partial \mathbf{V}}{\partial t} = -\nabla P + \mu^w \left( \Delta \mathbf{V} + \frac{1}{3} \nabla(\nabla \cdot \mathbf{V}) \right) + \mathbf{F},$$

$$\frac{\partial \rho^w}{\partial t} + \rho_0^w \nabla \cdot \mathbf{V} = 0 \quad \text{where } \rho_0 = \text{a constant},$$

$$P = c^2 \rho^w,$$

where  $\rho_0^w$  is a constant reference density. If we assume that  $\mu^w = 0$  then the system reduces to

$$\rho^w \frac{\partial \mathbf{V}}{\partial t} = -\nabla P + \mathbf{F}, \tag{27}$$

$$\nabla \cdot \mathbf{V} = -\frac{1}{\rho_0^w c^2} \frac{\partial P}{\partial t}, \tag{28}$$

which may be combined to form the equation:

$$-\Delta P + \nabla \cdot \mathbf{F} = -\frac{1}{c^2} \frac{\partial^2 P}{\partial t^2} \tag{29}$$

We now consider the time-harmonic case and assume  $P = p(x)e^{-i\omega t}$ ,  $\partial^2 P / \partial t^2 = -\omega^2 p(x)e^{-i\omega t}$ ,  $\nabla \cdot \mathbf{F} = (\nabla \cdot \mathbf{f})e^{-i\omega t}$ , from which we have

$$\Delta p + k^2 p = \phi, \quad \text{where } k^2 = \frac{\omega^2}{c^2}, \quad \text{and } \phi = \nabla \cdot \mathbf{f}.$$

The relationship between pressure may then be found using (27), i.e.

$$\frac{\partial \mathbf{V}}{\partial t} = \frac{1}{\rho^w} (-\nabla P + \mathbf{F}),$$

which for time-harmonic motion reduces to

$$\rho^w \omega^2 \mathbf{U}^w = (\nabla p - \mathbf{f}).$$

From this we get the interface condition

$$\rho^w \mathbf{n} \cdot \mathbf{U} = \frac{\partial p}{\partial n} - \mathbf{n} \cdot \mathbf{f}. \tag{30}$$

If  $\phi(\mathbf{x}) = \delta(\mathbf{x}, \mathbf{x}_0)$ , then we may choose

$$\mathbf{f}(\mathbf{x}) = \frac{1}{2\pi} \nabla_x \{ \log(\|\mathbf{x} - \mathbf{x}_0\|) - H(\mathbf{x}, \mathbf{x}_0) \}, \tag{31}$$

where  $H(\mathbf{x}, \mathbf{x}_0)$  is an arbitrary harmonic function. How we choose the harmonic function determines  $\mathbf{n} \cdot \mathbf{f}$  on the boundary. One possible choice is to take

$$\Gamma(\mathbf{x}, \mathbf{x}_0) := \frac{1}{2\pi} (\log(\|\mathbf{x} - \mathbf{x}_0\|) - H(\mathbf{x}, \mathbf{x}_0)),$$

as the Laplacian Green's function. This function vanishes on the boundary whose normal derivatives must be computed. Other choices are possible, i.e. the Laplacian Neumann function, whose normal derivative on the boundary is equal to  $(1/L)$ , where  $L$  is the perimeter of the boundary and whose Dirichlet boundary values must be computed, etc.

**Integral equations**

For the solution of Equation (10) in the water  $\Omega^w$ , we now employ the method of boundary integral equations. Let

$$G(\mathbf{x}, \zeta; k_0) := \frac{i}{4} H_0^{(1)}(k_0 \|\mathbf{x} - \zeta\|) \tag{32}$$

denote the fundamental solution of the Helmholtz equation with  $H_0^{(1)}$  being the modified Bessel function of the first kind. Then we may seek a solution of (10) in the form:

$$P(\mathbf{x}, \mathbf{x}_0) = \int_{\Omega^w} G(\mathbf{x}, \zeta; k_0) f(\zeta, \mathbf{x}_0) ds_\zeta - \int_{\Gamma} G(\mathbf{x}, \zeta; k_0) \phi(\zeta) ds_\zeta, \quad \mathbf{x} \in \Omega^w, \tag{33}$$

for fixed source point  $\mathbf{x}_0 \in \Omega^w$ , where  $f(\zeta, \mathbf{x}_0) = -q\delta(\zeta, \mathbf{x}_0)$  is the point source term. The first term on the right-hand side is the Newton potential which reduces to  $-qG(\mathbf{x}, \mathbf{x}_0; k_0)$ , while the second term is the simple-layer potential with the unknown density function  $\varphi$  to be determined. By the standard argument in potential theory [10], we arrive at the boundary integral equation of the first kind for the unknown density  $\varphi$ :

$$P(\mathbf{x}, \mathbf{x}_0) = -qG(\mathbf{x}, \mathbf{x}_0; k_0) - V\varphi(\mathbf{x}), \quad \mathbf{x} \in \Gamma, \tag{34}$$

where  $V$  is the simple-layer boundary integral operator defined by

$$V\varphi(\mathbf{x}) := \int_{\Gamma} G(\mathbf{x}, \zeta; k_0)\varphi(\zeta)ds_{\zeta}.$$

As was shown in [10],  $G(\mathbf{x}, \zeta; k_0)$  admits an asymptotic development

$$G(\mathbf{x}, \zeta; k_0) = G(\mathbf{x}, \zeta) - \frac{1}{2\pi}(\log(k_0 + \gamma_0) + S_{k_0}(\mathbf{x}, \zeta)),$$

where

$$\begin{aligned} \gamma_0 &= c_0 - \log 2 - i\frac{\pi}{2} \quad \text{with } c_0 = 0.5772 \text{ (Euler's constant),} \\ S_{k_0}(\mathbf{x}, \zeta) &= -\frac{1}{2\pi}(\log(k_0\|\mathbf{x} - \zeta\|) \sum_{m=1}^{\infty} a_m(k_0\|\mathbf{x} - \zeta\|)^{2m} \\ &\quad + \sum_{m=1}^{\infty} b_m(k_0\|\mathbf{x} - \zeta\|)^{2m}, \\ a_m &= \frac{-1}{2^{2m}(m!)^2}, \quad b_m = (\gamma_0 - 1 - 1/2 \cdots - 1/m)a_m. \end{aligned}$$

Here

$$G(\mathbf{x}, \zeta) = -\frac{1}{2\pi} \log \|\mathbf{x} - \zeta\|$$

is the fundamental solution for the Laplacian (or  $-\Delta$  rather). Based on the asymptotic development, it can be shown that

$$V\varphi(\mathbf{x}) = V_0\varphi(\mathbf{x}) + O(k_0 \log k_0^2), \quad \mathbf{x} \in \Gamma, \tag{35}$$

where

$$V_0\varphi(\mathbf{x}) := -\frac{1}{2\pi} \int_{\Gamma} \log(\|\mathbf{x} - \zeta\|)\varphi(\zeta)ds_{\zeta}.$$

This shows that for low frequency, we may approximate  $V$  by using  $V_0$  in order to simplify the computation as used in our numerical experiments.

In the same manner, by taking the normal derivative of the pressure  $P$  on  $\Gamma$ , we obtain a boundary integral equation of the second kind,

$$\left(\frac{1}{2}I - K'\right)\varphi = \frac{\partial}{\partial \mathbf{n}}P + q\frac{\partial}{\partial \mathbf{n}}G(\mathbf{x}, \mathbf{x}_0; k_0)|_{\Gamma}, \quad \mathbf{x} \in \Gamma, \tag{36}$$

where  $K'$  is the adjoint of the double-layer boundary integral operator given by

$$K'\varphi(\mathbf{x}) := \int_{\Gamma} \frac{\partial}{\partial \mathbf{n}_{\mathbf{x}}}G(\mathbf{x}, \zeta; k_0)\varphi(\zeta)ds_{\zeta}, \quad \mathbf{x} \in \Gamma.$$

Again  $K'$  can be approximated in terms of the corresponding adjoint operator for the Laplacian,

$$K'_0\varphi(\mathbf{x}) := \int_{\Gamma} \frac{\partial}{\partial \mathbf{n}_{\mathbf{x}}} G(\mathbf{x}, \zeta) \varphi(\zeta) \mathrm{d}s_{\zeta}, \quad \mathbf{x} \in \Gamma.$$

For interested readers, we refer the details to [11] and [10], where one may also find mapping properties of related boundary integral operators.